

SAXS and SANS investigations of Colloidal Dispersions of Magnetic Nanoparticles and Clay Nanoplatelets

F. L. O. PAULA,^a R. AQUINO,^a G. J. DA SILVA,^a J. DEPEYROT,^a F. A. TOURINHO,^b J.O. FOSSUM^{c*} AND K. D. KNUDSEN^d

^a*Complex Fluids Group. Institute of Physics. University of Braslia. Braslia. Brazil,*

^b*Complex Fluids Group. Institute of Chemistry. University of Braslia. Braslia.*

Brazil, ^cDepartment of Physics. Norwegian University of Science and Technology.

Hoegskoleringen 5. N-7491. Trondheim. Norway, and ^dPhysics Department. Institute for Energy Technology. Kjeller-Norway. E-mail: jon.fossum@ntnu.no

(Received 0 XXXXXXXX 0000; accepted 0 XXXXXXXX 0000)

Ferrofluids, Clays, Nanoparticles, Composite materials, SAXS, SANS

Abstract

We investigate mixed colloidal dispersion of clays platelets and magnetic nanoparticles using small angle scattering experiments; SANS and SAXS. Our results show that the contribution to the scattering essentially is due to the magnetic nanoparticles. The scattered intensities are proportional to the concentration of magnetic particles, indicating colloidal dispersion of non-interacting magnetic objects. The observed phase separation is characterized as a liquid-gas transition.

1. Introduction

It is a challenge in colloidal science to predict and monitor the thermodynamic stability of dispersions as well as associating theoretical models to experimental results. Several technological and industrial applications require a stable colloid which is directly related to the process of agglomeration and phase separation. Colloidal stability involves several kinds of particle interactions such as van der Waals attraction; electrostatic repulsion between electric double layers and in the case of ferrofluids, magnetic dipolar interactions. Considering the solvent as a continuous medium, it is possible to make analogies between colloidal and atomic systems, because the interparticle interaction potential have the same functional behavior for both cases (Israelachvili, 1985). In this context, liquid phases, gas phases and solid phases can be observed in colloidal dispersions. However in contrast to the atomic systems the interparticle interactions in a colloid can be controlled by certain experimental parameters such as the ionic strength, the temperature, the colloid pH and in particular for ferrofluids, the applied magnetic field. We study here a composite potentially smart material by associating two aqueous colloidal systems, namely the clay laponite solution and a ferrofluid, with the purpose of obtainin a magnetoreological product. Each one of these aqueous colloidal systems have their one phase behavior as a function of several parameters and strongly depend on the electrostatic interactions (Israelachvili, 1985). The magnetic nanoparticles used here i.e. the ferrofluid, have already been associated to other complex fluids such as liquid crystals (Matuo, 2002). The chemical synthesis (Tourinho, 1990) and the colloidal stability (Campos, 2001) of such magnetic nanoparticles in aqueous media are relatively well known and their phase behavior as a function of the ionic strength and temperature has been discussed using small angle neutron scattering (Dubois, 2000). Laponite (Fossum, 2000; Gabriel, 1996) platelets is a widely studied synthetic clay that belongs to the family of swelling 2:1 clays (Olphen,

1991). The colloidal phase diagram of aqueous Laponite suspensions as a function of the ionic strength and the concentration of laponite has been discussed and includes four different regions (phases): isotropic liquid, isotropic gel, nematic gel and flocculation. Recently maghemite magnetic nanoparticles were incorporated as a probe into clays dispersion in order to characterize their spatial repartition and microrheological behavior (Cousin, 2002). In this work we investigate the colloidal dispersion of clays platelets and magnetic nanoparticles using small angle scattering experiments. Clay Laponite dispersion (0.1 wt percent) is synthesized in the isotropic liquid phase and mixed with citrated ferrofluid based on cobalt ferrite nanoparticles in order to obtain a composite product. The parent laponite and ferrofluid colloids as well as mixed composites are investigated by small angle scattering experiments, which allow us to characterize the scattering objects in the composite samples as well as the colloidal stability of such laponite-ferrofluid composites.

2. Experimental

2.1. Aqueous suspensions of Laponite nanoplatelets

Laponite is a synthetic clay with general formula $\text{Si}_8\text{Mg}_{5.45}\text{Li}_{0.4}\text{H}_4\text{O}_{24}\text{Na}_{0.7}$, diameter around 25 nm and thickness of 1 nm and approximately monodisperse in size. The chemical pH stability range of laponite platelets solutions is narrow: below pH 9 the magnesium ions dissolve in solution and above pH 10 the dissolution of silica is observed (Thompson, 1992). The structural charge of the surface of the platelets is negative. The edge charge depends on the acid-base behavior of Si-OH and Mg-OH amphoteric hydroxyl groups which are the main species on the edge. Laponite powder with high chemical purity was purchased from Laporte Absorbents (UK). The Laponite stock solution was prepared in a sodium citrate solution with $[\text{Na}_3\text{Cit}] = 2.5 \times 10^{-3}$ mol L⁻¹ and vigorously stirred during 48 h.

2.2. Ferrofluid

Cobalt ferrite nanoparticle are obtained using a hydrothermal coprecipitating aqueous solution of a $CoCl_2 - FeCl_3$ mixture in alkaline medium (Tourinho, 1990). After the coprecipitation step these particles are conveniently peptized in an acidic medium by adjustment of the ionic strength resulting in an aqueous stable sol of high quality at $pH \approx 2$. Addition of trisodium citrate (Na3Cit) in the solution allows coating of the particles with citrate ions for dispersion in aqueous solution at $pH \approx 10$.

2.3. Synthesized Magnetic Nanoparticle Characterization

The structure morphology and mean size of our nanoparticles are determined through X-ray powder diffractogram and TEM pictures. The diffraction experiments were conducted at room temperature at the XRD Synchrotron beam line of the Brazilian Synchrotron Light Laboratory (LNLS) using a monochromatized 6.01keV ($\lambda = 2.0633\text{\AA}$) X-ray beam. Transmission Electron Microscopy (TEM) was done in a JEOL 100CX2 setup and allows to characterize the morphology and the size distribution of our nanoparticles.

2.4. Composite mixtures

Ionic strength and pH conditions to obtain a stable isotropic liquid dispersion of magnetic nanoparticles and laponite nanoplatelets are described elsewhere (Paula et.al 2006). Our composite materials are obtained by mixing an isotropic liquid dispersion of laponite at 0.1 percent w/w and a ferrofluid solution with a volume fraction of magnetic nanoparticles of 0.025 percent. In this case the number of platelets is around 5 times larger than the number of magnetic particles even if the amount of ferrite is about the amount of laponite.

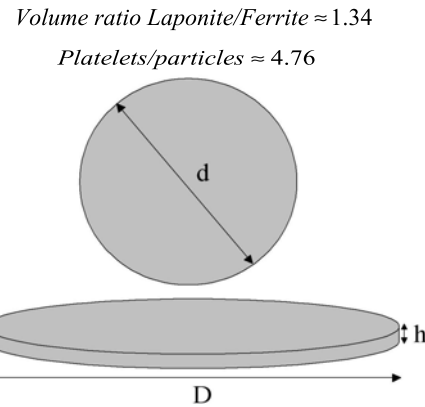


Fig. 1. Typical dimensions for a clay platelet ($h = 1$ nm, $D = 25$ nm) and a magnetic particle ($d = 14.0$ nm), as well as their volume ratio and concentration ratio (platelets/particles) in the composite material

2.5. SANS

The small angle neutron scattering (SANS) experiments were conducted at the SANS installation at the IFE reactor at Kjeller, Norway. The suspensions were filled in 1 mm quartz cuvettes. Each complete scattering curve is composed of 3 independent series of measurement, employing 3 different wavelength-distance combinations ($5.1\text{\AA}/1.0m$, $5.1\text{\AA}/3.4m$, $10.2\text{\AA}/3.4m$). By using these combinations a q -range from 0.008 to 0.2\AA^{-1} was covered. Standard reductions of the scattering data, including transmission corrections, were performed by incorporating data collected from empty cell, beam without cell, and blocked-beam background. When relevant, the data were transformed to an absolute scale (coherent differential cross section ($d\Sigma/d\Omega$)) by calculating the normalized scattered intensity from direct beam measurements. The respective scattering length densities (ρ) of CoFe_2O_4 nanoparticles, laponite platelets, water and sodium citrate are $6.2 \times 10^{10} \text{ cm}^{-2}$, $4.1 \times 10^{10} \text{ cm}^{-2}$, $-0.53 \times 10^{10} \text{ cm}^{-2}$ and $2.0 \times 10^{10} \text{ cm}^{-2}$. Here, the scattering of neutrons by magnetic ferrite nanoparticles is mainly due to nuclear interactions with all nuclei of the sample(Gazeau, 2003).

2.6. SAXS

The small angle X-Ray scattering (SAXS) experiment was done on beamline D11A-SAXS at the Laboratorio Nacional de Luz Sincrotron (LNLS) in Campinas, Brazil (energy range 6-12 keV). All data were collected at a wavelength of 1.756\AA with the sample to image plate detector distance of 1.500 m. The samples were filled in 1 mm quartz capillary. Data treatment was performed using the software FIT2D (ESRF) with usual corrections included in its routine. The output of this software provides the corrected intensities in order to subtract the scattering from the citrated solution and the quartz capillary.

3. SAS analysis

The scattered intensity of a diluted dispersion can be written as a function of the scattering vector $I(q) = nV^2\Delta\rho^2P(q)$ where n is the number of scattering objects of average volume V per volume unit (cm^{-3}) of solution, $\Delta\rho$ is the contrast between the particles and the solvent and $P(q)$ is the particle form factor proportional to the square modulus of the particle structure factor ($P(q) = |F(q)|^2$). At lower q , the scattering is described by the Guinier law(Guinier, 1955) and allows to determine the gyration radius of the scattering object R_g by writing the low q expansion of the scattering intensity $I(q) = I(0) \exp\left(-q^2R_g^2/3\right)$. At high values of q , the scattering curve reflects the characteristics of the interface between the scattering object and the solvent (Porod region). In the case of platelets ($h \ll D$) the measured scattering intensity scales with q^{-2} as a characteristic feature for scattering of randomly oriented discs (Ramsay, 1990). In the case of spheroidal particles, the scattering intensity in the Porod regime scales with q^{-4} .

Magnetic nanoparticles of ferrofluids are always polydisperse, and the mathematical function which best describes the size distribution is a lognormal law of particles radii:

$$P(R) = \frac{1}{R\sigma\sqrt{2\pi}} \exp \left[-\frac{\ln^2(R/R_0)}{2\sigma^2} \right] \quad (1)$$

where R_0 is the characteristic radius of the distribution given by $\ln R_0 = \langle \ln R \rangle$, σ is the standard deviation or polydispersity index. The n^{th} moment of the log-normal distribution are defined by $\langle R^n \rangle = \int R^n P(R) d(R) = R_0^n \exp(n^2\sigma^2/2)$. In such context, we can use a global scattering function proposed by G. Beaucage (Beaucage, 1995) to write the scattering intensity in the case of a lognormal distribution of spherical particles:

$$I(q) = Ge^{(-qR_g^2/3)} + B \left\{ \frac{\operatorname{erf} \left(qR_g/\sqrt{6} \right)^3}{q} \right\}^4 + y_0 \quad (2)$$

where $\operatorname{erf}(x)$ is the error function, G is the Guinier pre-factor proportional to the concentration of scattering objects and to the square of the volume, B is a constant pre-factor specific to the kind of power law obtained for high q values, and y_0 is a term introduced in order to take into account the incoherent scattering. In the case of a lognormal distribution the parameters R_g and B are related to the characteristic radius and the polydispersity index by:

$$R_g = \sqrt{\frac{3}{5}} \exp 7\sigma^2 R_0 \quad (3)$$

$$B = G \frac{9e^{-14\sigma^2}}{2R_0^4} \quad (4)$$

The parameters R_0 , σ , G and y_0 are deduced by fitting the small angle scattering curves to equation 2 through a non linear least square fitting procedure with a statistical weighting.

4. Results and discussion

Figure 2 displays the obtained powder diffractogram for our synthesized cobalt ferrite magnetic nanoparticles. The position and relative intensities of the diffracted lines are characteristic of the spinel crystallographic structure. The average radius is determined according to the Scherrer equation using the half width of the stronger diffraction peak and is equal to 7.0 nm. The inset of Figure 2 presents a typical TEM picture of the same sample and as it can be seen the nanoparticles are approximately spherical and polydisperse. Counting about 500 individual particles allows to obtain the size histogram that is fitted by a lognormal law of parameters $R_0 = 5.5\text{nm}$ and $\sigma = 0.3$.

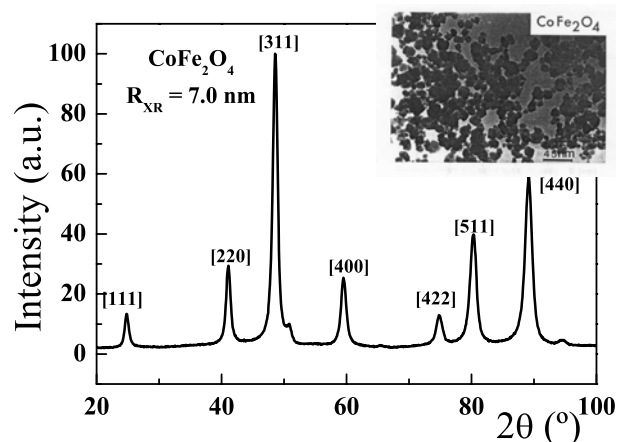


Fig. 2. XRD powder diffractogram of synthesized cobalt ferrite nanoparticles. The inset displays a TEM picture of the same sample.

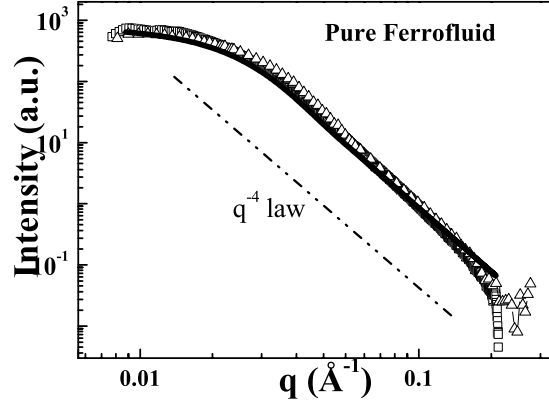


Fig. 3. Observed SANS (triangles) and SAXS (squares) scattering from pure $\phi = 1\%$ citrated cobalt ferrite ferrofluid. The dashed line is a guide line indicating the slope -4 . The full line is the best fit to the SAXS data using the equation 2.

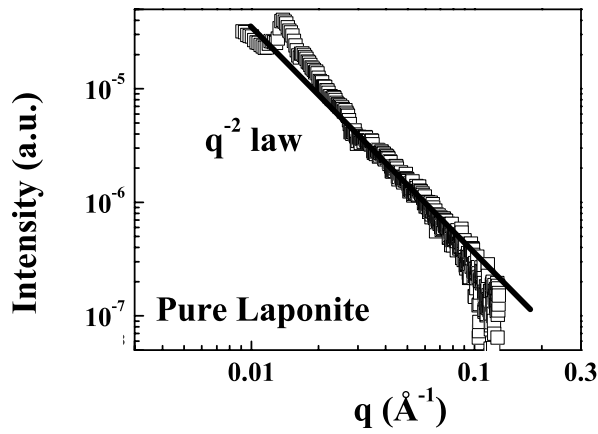


Fig. 4. Observed SAXS scattering from the pure dilute laponite solution, 0.1 percent by weight. The full line is a guide line indicating q^{-2} behaviour.

Figure 3 presents the log-log plot of SANS and SAXS intensities of our pure dilute citrate ferrofluid ($\phi = 1\%$) as a function of the scattering vector. Both measurements collapse on a same master curve using a normalization scaling factor in between the SAXS and SANS data sets. In both case the scattering intensity is proportional to the

volume fraction of magnetic nanoparticles suggesting a non-interacting regime. For smaller values of the scattering vector, q , typically $q < 0.01$, the scattering shows a plateau also indicating the absence of aggregates and interactions between scattering objects. For larger q values, the scattering intensity scales well with q^{-4} , indicating as expected that the scattering objects are spheroidal ones. The full line in Figure 3 represents the best fit obtained using equation 2 and the deduced values of the lognormal size distribution parameters are $R_0 = 5.52\text{nm}$ and $\sigma = 0.326$.

Figure 4 shows SAXS scattering from the 0.1% w/w laponite dispersion used in the composite with a ionic strength (I) of $1.5 \times 10^{-3} \text{ mol L}^{-1}$. In such conditions the clay dispersion is an isotropic liquid phase. The full line in Fig. 4 shows that the scattered intensity from our laponite dispersion is close to a q^{-2} behavior as expected for a solution of randomly oriented platelets.

The laponite-ferrofluid composite sample presents phase separation under an applied field of approximately 12kG, using a discoid rare earth permanent magnet. The composite separates in a diluted phase of magnetic nanoparticle (upper phase) and a more concentrated one (lower phase). Figure 5 and 6 presents the log-log plot of the scattered intensities of the diluted and concentrated phase of the composite sample. The scattered intensity from pure laponite platelets at our concentration (0.1 percent by weight) is smaller by several orders of magnitude as compared to the scattering obtained from magnetic nanoparticles. Moreover the slope of the high q region follows a q^{-4} law as expected in the Porod region for non-interacting spheroidal particles. These results clearly indicate that the scattering from our laponite-ferrofluid composite is mainly due to the magnetic nanoparticles, both for SAXS and for SANS. Thus we use equation 2 to determine the parameters G , R_0 , σ and y_0 . The resultant fitted parameters are collected in Table I for diluted and more concentrated phase. The fitted values for R_0 and σ in both case well agree with those determined for the

diluted pure ferrofluid showing that for our composite sample, the scattering object is the same for both phases. The inset of Fig. 5 and 6 display the low q region and the full line is the linear fitting with the Guinier Law giving a R_g value (related to R_0 by equation 3) in a good agreement with R_0 obtained from the fit with the global scattering function. The obtained R_0 and σ compare well with the R_{XR} value using the following empirical relationship $R_{XR} = R_0 e^{2.5\sigma^2}$ (Tronc, 1985). From the ratio between the G values. we are able to estimate the concentrations of the diluted and the more concentrated phases equal to 0.01% and 0.015% respectively. The SANS data have been multiplied with a factor to fit with the SAXS data in the middle- q -region, and we find relatively more incoherent scattering (at high q) for neutrons compared to x-rays, and also that the incoherent SANS scattering scales in the same manner as the coherent SANS scattering with respect to particle concentration, i.e. proportional to the number of scatterers.

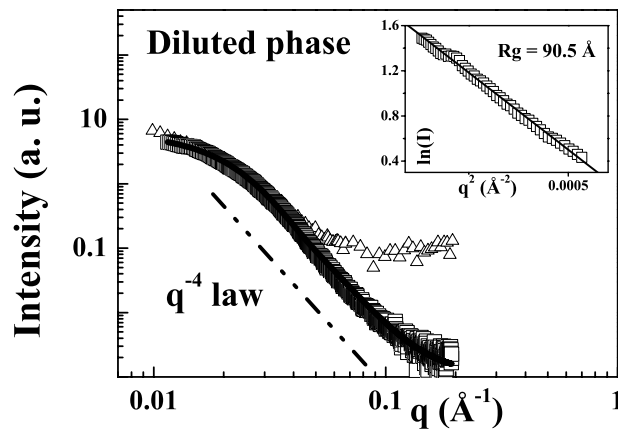


Fig. 5. Observed SANS (triangles) and SAXS (squares) scattering curves from the dilute phase of the composite sample. The dashed line is a guide line indicating the slope -4 , and the full line is the best fit using the equation 2. The inset displays the low q region where the full line is a fit to the Guinier law

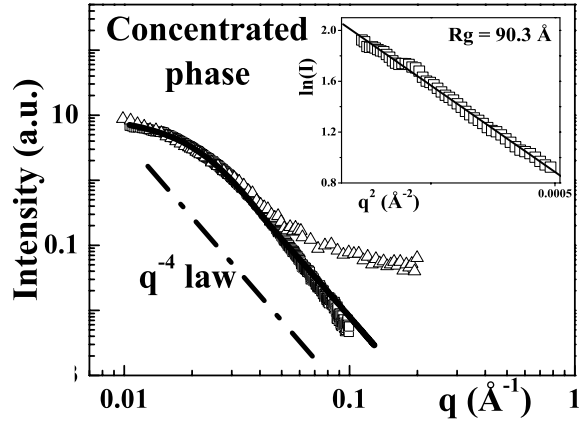


Fig. 6. Observed SANS (triangles) and SAXS (squares) scattering from the concentrated phase of the composite sample. The dashed line is a guide line indicating the slope -4 , and the full line is the best fit using the equation 2. The inset displays the low q region where the full line is a fit to the Guinier law

Table 1. *Fitparameters for the two phases of the composite*
 Fitparameters Diluted phase Concentrated phase

	Diluted phase	Concentrated phase
G	6.30 ± 1.15	9.6 ± 1.1
R_0	$5.79 \pm 0.20 \text{ nm}$	$5.86 \pm 0.30 \text{ nm}$
σ	0.32 ± 0.06	0.33 ± 0.06
y_0	0.0012	0.0000

5. Conclusions

A composite material was obtained from the mixture of an isotropic phase laponite solution with a diluted citrate ferrofluid for a given magnetic nanoparticle volume fraction. Such a laponite-ferrofluid composite material touches general questions concerning colloidal stability. During sample mixing, the pH and ionic strength parameters of the final product were optimized in order to respect the interval of stability of each component. Small angle scattering experiments were performed in order to investigate the nanostructure of the composite sample. The scattering is much more intense for the magnetic nanoparticles than for the laponite platelets, which implies that the

composite scattering signal is mainly due to the magnetic nanoparticles. The scattering obtained by SANS and SAXS collapse in a master curve, but differs at high q where incoherent scattering is observed in SANS. In both cases, SAXS and/or SANS, the scattered intensity is proportional to the volume fraction of magnetic particles present on each phase, and this indicates a non interacting particle system for both phases. Fitting the scattered intensities to a global scattering function including the size polydispersity allows us to deduce the characteristic radius and polydispersity index of the scattering object present in the composite sample, and to show that is the same as for the pure ferrofluid sample.

Acknowledgements The authors wish to acknowledge the help from the staff at the beamline D11A-SAXS at the Laboratorio Nacional de Luz Sincrotron (LNLS) during the SAXS experiments. This work was supported by the Research Council of Norway (RCN) through the NANOMAT Program: RCN project numbers 152426/431, 154059/420 and 148865/432, as well as 138368/V30 and SUP154059/420.

References

Beaucage, G. (1995). *J. Appl. Cryst.* **28**, 717.

Campos, A. F. C. & Tourinho, F. A. & Silva, G. J. da & Lara, M. C. F. L. & Depeyrot, J. (2001). *Eur. Phys. J. E.* **6**, 29.

Cousin, F. & Cabuil, V. & Levitz, P. (2002). *Langmuir* **18**, 1466.

Dubois, E. & Perzynski, R. & Bou, F. & Cabuil, V. (2000). *Langmuir* **16**, 5617.

Fossum, J-O. (2000). in: *Soft Condensed Matter: Configurations, Dynamics, and Functionality* Netherlands: Kluwer Academic.

Gabriel, J. P. C. & Sanchez, C. & Davidson, P. (1996). *J. Phys. Chem.* **100**, 11139.

Gazeau F. & Boue F. & Dubois & Perzynski R. (2003). *J. Phys. Chem.* **15**(15), S1305.

Guinier, A. & Fournet, G. (1995). *Small-Angle Scattering of X-rays* New York: Wiley.

Israelachvili, J. N. (1985). *Intermolecular and Surface Forces* New York: Academic Press.

Matuo, C. Y. & Tourinho, F. A. & Sousa, M. H. & Depeyrot, J. & AFigueiredo Neto., A. M. (2002). *Braz. J. Phys.* **32**, 458.

Mourchid, A.& Lecolier, E.& Damme, H. van& Levitz, P.& (1998) *Langmuir* **14**, 4718.

Olphen, H. van. (1991) *An introduction to Clay Colloid Chemistry* Florida: Krieger Publishing Company.

Paula F. L. O.& Depeyrot J.& da Silva G. J.& Aquino R.& Tourinho F. A.& Fossum J. O.& Knudsen K.D. *Work in progress*

Ramsay, J. D. F.& Swanton, S. W. & Bunce, J.,(1990). *J. Chem. Soc. Faraday Trans.* **86**, 3919.

Thompson, D. W. & Butterworth, T, J.(1992). *Colloid Interface Sci.* **151**(1), 236.

Tourinho, F. A.& Franck, R. & Massart, R.(1990). *J. Mater. Sci.* **25**, 3249.

Tronc, E. & Bonnin, D. (1985). *J. Phys. Lett.* **46**, L437.

Synopsis

Supply a synopsis of the paper for inclusion in the Table of Contents.
